Supporting information for

Suppression of nonradiative transitions of triplet excitons via fused/non-fused strategy for realizing efficient room-temperature phosphorescence

Haiyang Shu[a, b], Yulu Liu[a, b], Liang Chen[a, b], Zhiqiang Chen[a, b], Xin Wang[a, b], Xiaofu Wu[a], Hui Tong[*a, b] Lixiang Wang [*a, b]

[a] State Key Laboratory of Polymer Physics and Chemistry, Changchun Institute of Applied Chemistry, Chinese Academy of Sciences, Changchun 130022, China
[b] School of Applied Chemistry and Engineering, University of Science and Technology of China, Hefei 230026, China

Corresponding Author
* E-mail: chemtonghui@ciac.ac.cn; lixiang@ciac.ac.cn

Table of contents

Page

1. Experimental details

General information: ^{1}H-NMR and ^{13}C-NMR spectra were measured using a Bruker Avance NMR spectrometer at 25°C unless noted. Gas chromatography-mass spectrometry (GC-MS) was measured with agent 5975. Matrix-assisted laser desorption/ ionization time of flight (MALDI-TOF) mass spectra were measured on AXIMA CFR MS apparatus (COMPACT).

Photophysical measurements: UV/Vis absorption spectra were measured by a Perkin–Elmer Lambda 35 UV/Vis spectrometer. Photoluminescence (PL) measurements were conducted utilizing FluoroMax-4 spectrophotometer equipped with a 150 W xenon lamp as the excitation source. The quantum yields were measured on an integrating sphere (Hamamatsu Photonics C9920-2). Fluorescence lifetimes and phosphorescence lifetimes were measured with an Edinburgh FLSP-980 fluorescence spectrophotometer. Fluorescence lifetime is using picoseconds pulsed lasers (EPLSs) as the excitation source and time correlated single photon counting (TCSPC) as data acquisition technique. Phosphorescence lifetime is using a 60 W xenon flashlamp (μF2) as the excitation source and multi-channel scaling (MCS) for time resolved photon counting as data acquisition technique.

Synthesis: All the materials used for the synthesis were purchased from commercial sources without further purification unless noted. Solvents for chemical synthesis were purified according to standard procedures.
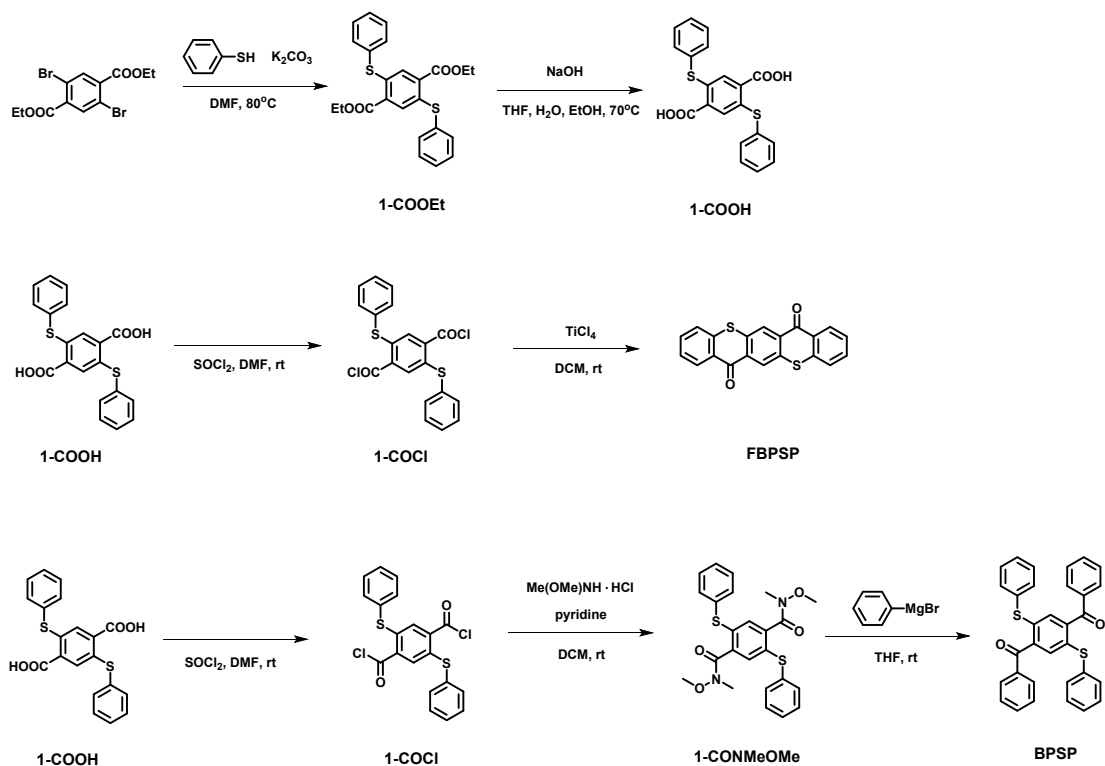
Scheme S1. Synthetic routes of the target compounds.

Diethyl 2,5-bis(phenylthio)terephthalate (1-COOEt)

Sodium thiophenate (5.0 mmol, 0.66 g) was added to a solution of diethyl 2,5-dibromoterephthalate (1.0 mmol, 0.38 g) in dimethylformamide (DMF) (15 mL) under argon. The reaction system was reacted at 80°C for 2 h. After cooling to room temperature, deionized water was added and stirred for 30 minutes. The mixture was filtered and the filter cake was collected. The crude product was purified by silica gel column chromatography (petroleum ether and dichloromethane) to afford the product as a white solid (0.40 g, 90%). ^{1}H NMR (500 MHz, CDCl3) δ 7.55 – 7.49 (m, 4H), 7.46 – 7.39 (m, 8H), 4.23 (q, J = 7.1 Hz, 4H), 1.20 (t, J = 7.1 Hz, 6H). MALDI TOF-MS: calcd for $C_{24}H_{22}O_4S_2$ [M]$^+$: 438.1; found: 438.1.

2,5-bis(phenylthio)terephthalic acid (1-COOH)

Tetrahydrofuran (THF) (10 mL), ethanol (10 mL) and H_2O (5 mL) were added to a two-neck bottle containing 1-COOEt (2 mmol, 0.88 g) and NaOH (40 mmol, 1.60 g) under argon. The solution was heated at 70°C overnight. After cooling to room temperature, the mixture was acidified to pH=1 by 2 M HCl and stirred for 30 minutes. The target carboxylic acid 1-COOH (0.73 g, 95%) was collected via suction filtration and was dried under vacuum and directly used in the next step without further purification. ^{1}H NMR (500 MHz, DMSO) δ 13.41 (s, 2H), 7.57 – 7.48 (m, 10H), 7.31 (s, 2H). MALDI TOF-MS: calcd for $C_{20}H_{14}O_4S_2$ [M]$^+$: 382.0; found: 382.0.

Thiochromeno[2,3-b] thioxanthene-7,14-dione (FBPSP)

A solution of phthalic acid 1-COOH (1.00 mmol, 0.38 g) in DMF (0.5 mL) and thionyl chloride (10 mL) was stirred for 4 h at room temperature, before all volatile substances were removed under reduced pressure. After a solution of titanium tetrachloride (10 mmol, 3.0 mL) in dichloromethane (20 mL) was added, the resulting reaction mixture was stirred for 16 h at room temperature. Then, the reaction mixture was poured into water (20 mL) and the organic layer was extracted with dichloromethane. The combined organic layers were dried over anhydrous sodium sulfate, filtered, and dried under reduced pressure. The crude product was purified by silica gel column chromatography (petroleum ether and chloroform) to afford the product as an orange solid (0.40 g, 90%). ^{1}H NMR (500 MHz, CDCl$_3$) δ 8.88 (s, 2H), 8.64 (dd, J = 8.1, 1.3 Hz, 2H), 7.71 – 7.66 (m, 2H), 7.66 – 7.62 (m, 2H), 7.55 – 7.50 (m, 2H). ^{13}C NMR (101 MHz, C$_2$D$_2$Cl$_4$) δ 179.19, 137.81, 134.23, 133.01, 131.48, 130.23, 129.30, 128.06, 126.68, 126.31. GC-MS (m/z) calcd for C$_{20}$H$_{10}$O$_2$S$_2$ [M]$^+$: 346; Found: 346.

N^1, N^4-dimethoxy-N^1, N^4-dimethyl-2,5-bis(phenylthio)terephthalamide (1-CONMeOMe)

A solution of phthalic acid 1-COOH (5 mmol, 1.91 g) in DMF (0.5 mL) and thionyl chloride (50 mL) was stirred for 4 h at room temperature, before all volatile substances were removed under reduced pressure. Then, N-methoxy-N-methylamine hydrochloride (15 mmol, 1.47 g) and CH$_2$Cl$_2$ (50 mL) were added under argon atmosphere. The mixture was cooled to 0°C, and pyridine (30 mmol, 2.37 g) was added dropwise. The resulting mixture was stirred at room temperature for 2 h before quenching with water (50 mL). The aqueous layer was extracted with CH$_2$Cl$_2$. The combined organic layer was washed with 1 M HCl aq. (50 mL) and sat. aq. NaCl solution (50 mL), dried over Na$_2$SO$_4$. The crude product was purified by silica gel column chromatography (petroleum ether and ethyl acetate) to afford the product as a white solid (1.64 g, 70%). ^{1}H NMR (400 MHz, CDCl$_3$) δ 7.46-7.37 (m, 4H), 7.37 – 7.23 (m, 6H), 7.13 (s, 2H), 3.42 (s, 3H), 3.25 (s, 3H). MALDI TOF-MS: calcd for C$_{24}$H$_{24}$N$_2$O$_4$S$_2$ [M]$^+$: 468.1; found: 468.1.

(2,5-bis(phenylthio)-1,4-phenylene) bis(phenylmethanone) (BPSP)

A solution of 1-CONMeOMe (2 mmol, 0.94 g) in THF (50 mL) was stirred for 0.5 h at 0°C. Bromophenylmagnesium (1 M in THF, 3 mL) was added dropwise. The resulting mixture was stirred at room temperature for 6 h before quenching with 1 M HCl aq. (50 mL). The aqueous layer was extracted with CH$_2$Cl$_2$ and the combined layer was washed with sat. aq. NaHCO$_3$ and sat. aq. NaCl, dried over Na$_2$SO$_4$. The crude product was purified by silica gel column chromatography (petroleum ether and dichloromethane) to afford the product as a yellow solid (1.00 g, 85%). ^{1}H NMR (500 MHz, CDCl$_3$) δ 7.72 (dd, J = 8.3, 1.2 Hz, 4H), 7.59 – 7.54 (m, 2H), 7.43 – 7.38 (m, 4H), 7.36 – 7.32 (m, 4H), 7.26 – 7.23 (m, 6H), 7.23 (s, 2H). ^{13}C NMR (126 MHz, CDCl$_3$) δ 195.09, 140.61, 136.38, 135.47, 133.52, 133.43, 133.01, 131.61, 130.08, 129.51, 128.52, 128.38. MALDI TOF-MS: calcd for C$_{32}$H$_{22}$O$_2$S$_2$ [M]$^+$: 502.1; found: 502.1.

2.Photophysical measurements
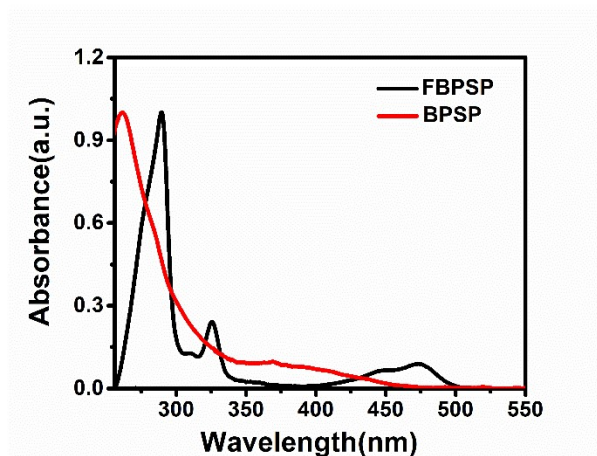
Fig. S1 UV-vis spectra of FBPSP and BPSP in THF solution at room temperature (10 μM).

The radiative rate constant of phosphorescence (k_r^P), the sum of the nonradiative constant of phosphorescence and the quenching rate of T_1 phosphorescence ($k_{nr}^P + k_q$) of BPSP and FBPSP were calculated according to the following equations:

$$\Phi_{FL} = 1 - \Phi_{ISC} - \Phi_{nr}^F \tag{S1}$$

$$\Phi_{Ph} = \Phi_{ISC} - \Phi_{nr}^P - \Phi_q \tag{S2}$$

$$k_{ISC} = \frac{\Phi_{ISC}}{\tau_{FL}} \tag{S3}$$

$$\frac{1}{\tau_{Ph}} = k_r^P + k_{nr}^P + k_q \tag{S4}$$

$$\Phi_{Ph} = \frac{\Phi_{ISC}k_r^P}{k_r^P + k_{nr}^P + k_q} \tag{S5}$$

Where Φ_{Ph} is the absolute quantum yield of phosphorescence, and τ_{Ph} is the average lifetime of phosphorescence.[1-3]

Table S1. Summary of photophysical parameters of FBPSP and BPSP in solution.

	λ_F (nm)	τ_F (ns)	Φ_F (%)	λ_P (nm)	τ_P (μs)	Φ_P (%)	k_r^p (10^3 s^{-1})	$k_{nr} + k_q$ (10^5 s^{-1})
FBPSP	393	5.76	0.1	488	1.25	0.6	5.00	8.28
BPSP	400	5.75	0.1	-	-	-	-	-

Table S2. Summary of photophysical parameters of FBPSP and BPSP in doped film.

	λ_F (nm)	τ_F (ns)	Φ_F (%)	λ_P (nm)	τ_P (ms)	Φ_P (%)	k_r^p (10^2 s^{-1})	$k_{nr} + k_q$ (s^{-1})
FBPSP	-	-	-	488	24.75	47.0	0.19	21.41
BPSP	498	3.16	0.7	540	0.30	0.3	0.10	3.32×10^3

Table S3. Summary of photophysical parameters of FBPSP and BPSP in crystalline state.

|	λ_F (nm)	τ_F (ns)	Φ_F (%)	λ_P (nm)	τ_P (ms)	Φ_P (%)	k_r^p (10^2 s^{-1})	$k_{nr} + k_q$ (10^2 s^{-1})
FBPSP	-	-	-	555	5.00	2.3	0.05	1.95
BPSP	510	3.21	10.9	550	0.87	6.9	0.79	10.70

3. X-ray crystallographic analysis

The single crystal of FBPSP was cultivated by the solvent diffusion method in chloroform and methanol. The single crystal of BPSP was cultivated by the solvent diffusion method in dichloromethane and hexane. The single crystal X-ray diffraction experiments were carried out using a Bruker Smart APEX diffractometer with a CCD area detector and graphite monochromator, Mo Kα radiation (λ =0.71073 Å). The intensity data were recorded with ω scan mode. Lorentz, polarization factors were made for the intensity data and absorption corrections were performed using SADABS program. The crystal structure was determined using the SHELXTL program and refined using full matrix least squares. All non-hydrogen atoms were assigned with anisotropic displacement parameters, whereas hydrogen atoms were placed at calculated positions theoretically and included in the final cycles of refinement in a riding model along with the attached carbons. Thus, obtained crystallographic parameters of FBPSP and BPSP were summarized in Table S4 and CCDC reference number are 2174907 and 2174799.

Table S4. Single crystal data of FBPSP and BPSP.

Compound	FBPSP	BPSP
Empirical formula	$C_{20}H_{10}O_2S_2$	$C_{32}H_{22}O_2S_2$
Formula weight	346.4	502.65
Temperature	193 K	299 K
Crystal system	Monoclinic	Monoclinic
Space group	$P2_1/c$	$P2_1/n$
Unit cell dimensions	a=7.932(2) Å	a=5.4922 (2) Å
	b=3.8700(7) Å	b=20.1526 (8) Å
	c=23.646(4) Å	c=11.5308(5) Å
	$\alpha = 90°$	$\alpha = 90°$
	$\beta = 92.506(9)°$	$\beta = 100.273(1)°$
	$\gamma = 90°$	$\gamma = 90°$
Volume (Å^3)	725.2(3)	1255.79(9)
Z	2	2
Density (g/cm^3)	1.586	1.329
F (000)	356.0	524.0
2θ range for data collection	2.57 to 36.90°	3.59 to 34.86°
Data/restraints/parameters	11171/1283/209	43636/3302/163
Goodness-of-fit on F^2	1.126	1.023
Final R indexes [all data]	$R_1 = 0.0603$, $wR_2 = 0.1706$	$R_1 = 0.0542$, $wR_2 = 0.1572$
Largest diff. peak and hole	0.45 and -0.55 e Å^{-3}	0.46 and -0.47 e Å^{-3}
CCDC	2174907	2174799

4. Theoretical calculation results

Density functional theory (DFT) and time-dependent DFT (TD-DFT) calculations were carried out at the M06-2x/def2-SV level using Gaussian 09 package.[4] BPSP and FBPSP were directly optimized to obtain the S_0 geometry and T_1 geometry. The TDDFT calculations for all molecules are performed using the optimized S_0 geometry. The analysis of spin density distribution (SDD) of triplet excitons was carried out by Multiwfn 3.7 and was renderings by VMD 1.9.3.[5,6] The Huang-Rhys (HR) factors for $T_1 \rightarrow S_0$ transition were conducted with the DUSHIN module in MOMAP (Molecular Materials Property Prediction Package).[7,8] The representative vibration modes were renderings by VMD 1.9.3.
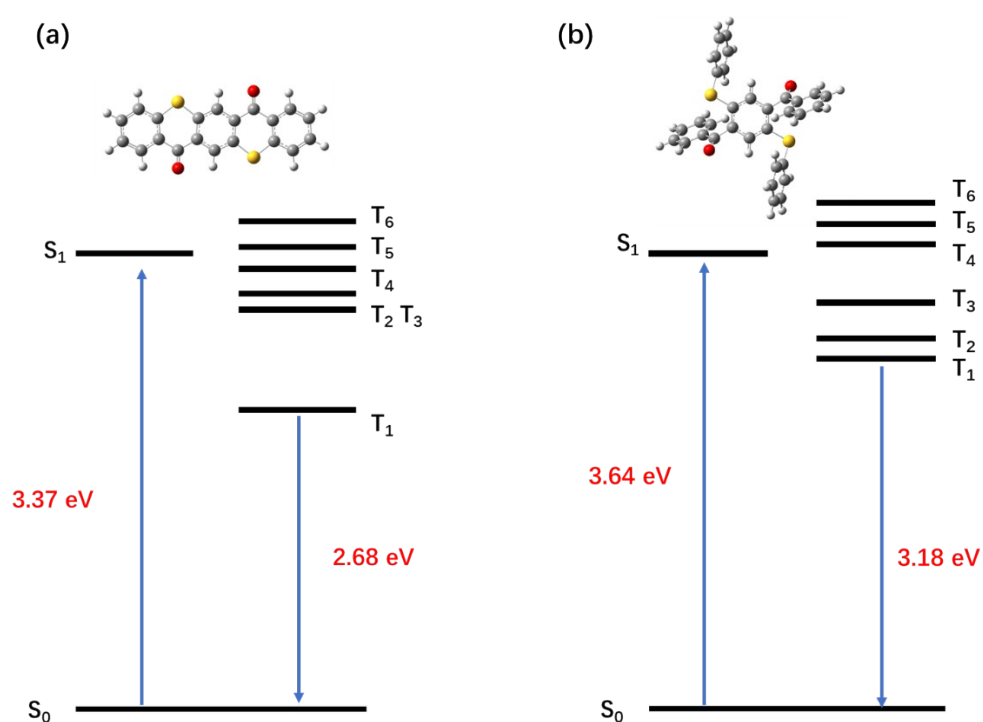
Fig. S2 TD-DFT calculated energy levels for (a) FBPSP and (b) BPSP at the optimized S_0-geometry.

Table S5. The singlet and triplet excited state energies of FBPSP at the optimized S_0-geometry. $T_n < S_1 + 0.3$ eV were marked in light green.

Excited state	Energy (eV)	Energy gap (S_1-T_n) (eV)
S_1	3.3737	
T_1	2.6783	0.6954
T_2	3.3052	0.0685
T_3	3.3052	0.0685
T_4	3.3282	0.0455
T_5	3.4556	-0.0819
T_6	3.6333	-0.2596
T_7	3.9000	-0.5263

Table S6. The singlet and triplet excited state energies of BPSP at the optimized S_0-geometry. $T_n < S_1 + 0.3$ eV were marked in light green.

| Excited state	Energy (eV)	Energy gap (S_1-T_n) (eV)
S_1	3.6412	
T_1	3.1816	0.4596
T_2	3.2308	0.4104
T_3	3.4645	0.1767
T_4	3.7135	-0.0723
T_5	3.7476	-0.1064
T_6	3.8097	-0.1682
T_7	3.9809	-0.3397
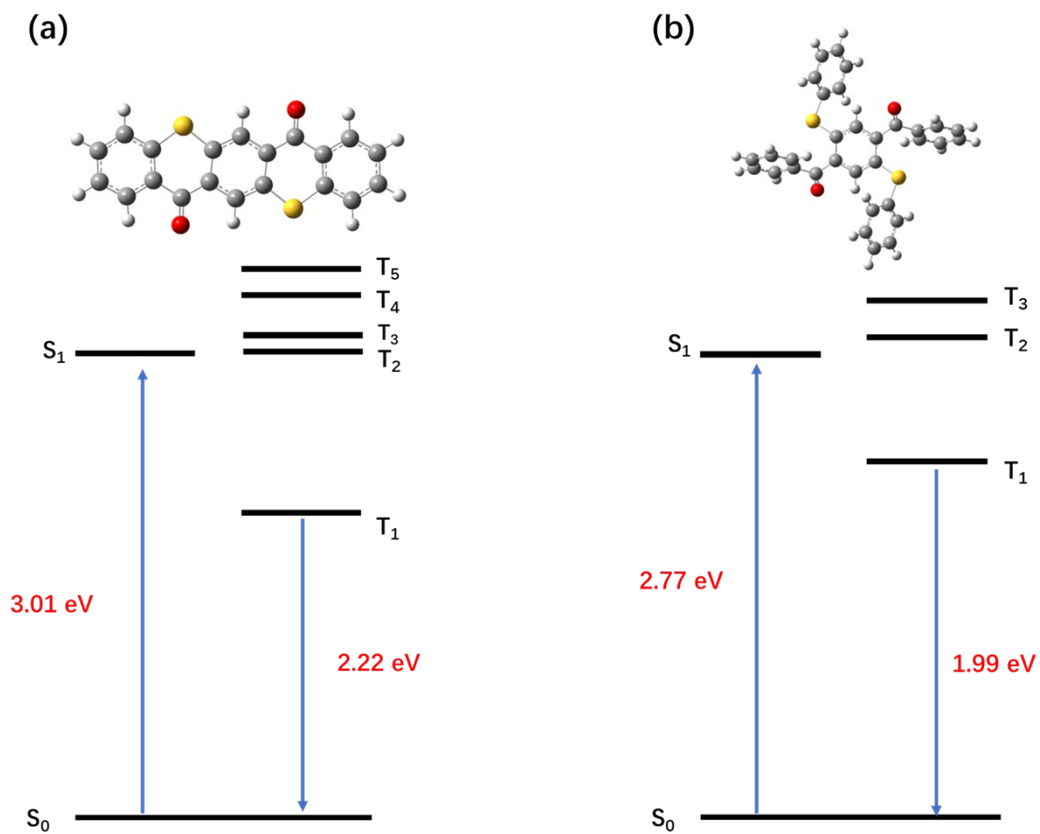
Fig. S3 TD-DFT calculated energy levels for (a) FBPSP and (b) BPSP at the optimized T_1-geometry.

Table S7. The singlet and triplet excited state energies of FBPSP at the optimized T_1-geometry. $T_n < S_1 + 0.3$ eV were marked in light green.

Excited state	Energy (eV)	Energy gap (S_1-T_n) (eV)
S_1	3.0067	
T_1	2.2150	0.7917
T_2	3.1175	-0.1108
T_3	3.1359	-0.1292
T_4	3.1635	-0.1568
T_5	3.2350	-0.2283
T_6	3.5051	-0.4984

Table S8. The singlet and triplet excited state energies of BPSP at the optimized T_1-geometry. $T_n < S_1 + 0.3$ eV were marked in light green.

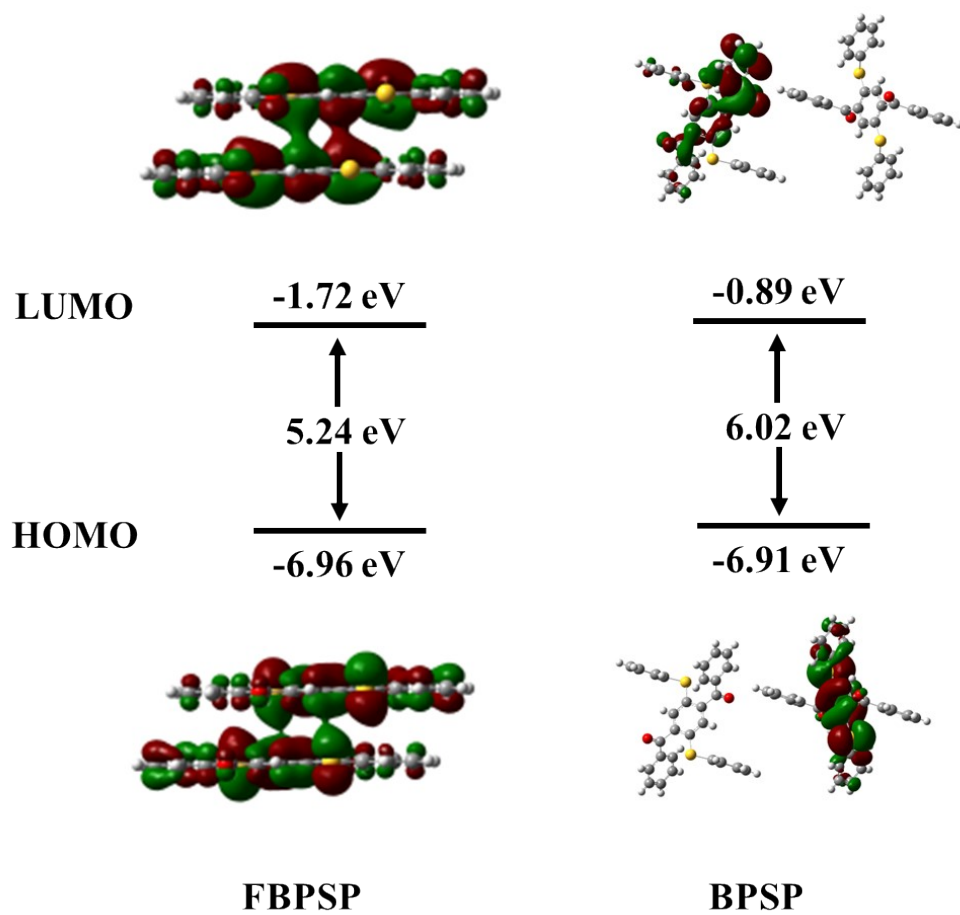| Excited state	Energy (eV)	Energy gap (S_1-T_n) (eV)
S_1	2.7705	
T_1	1.9897	0.7808
T_2	2.8960	-0.1255
T_3	2.9464	-0.1759
T_4	3.4077	-0.6302
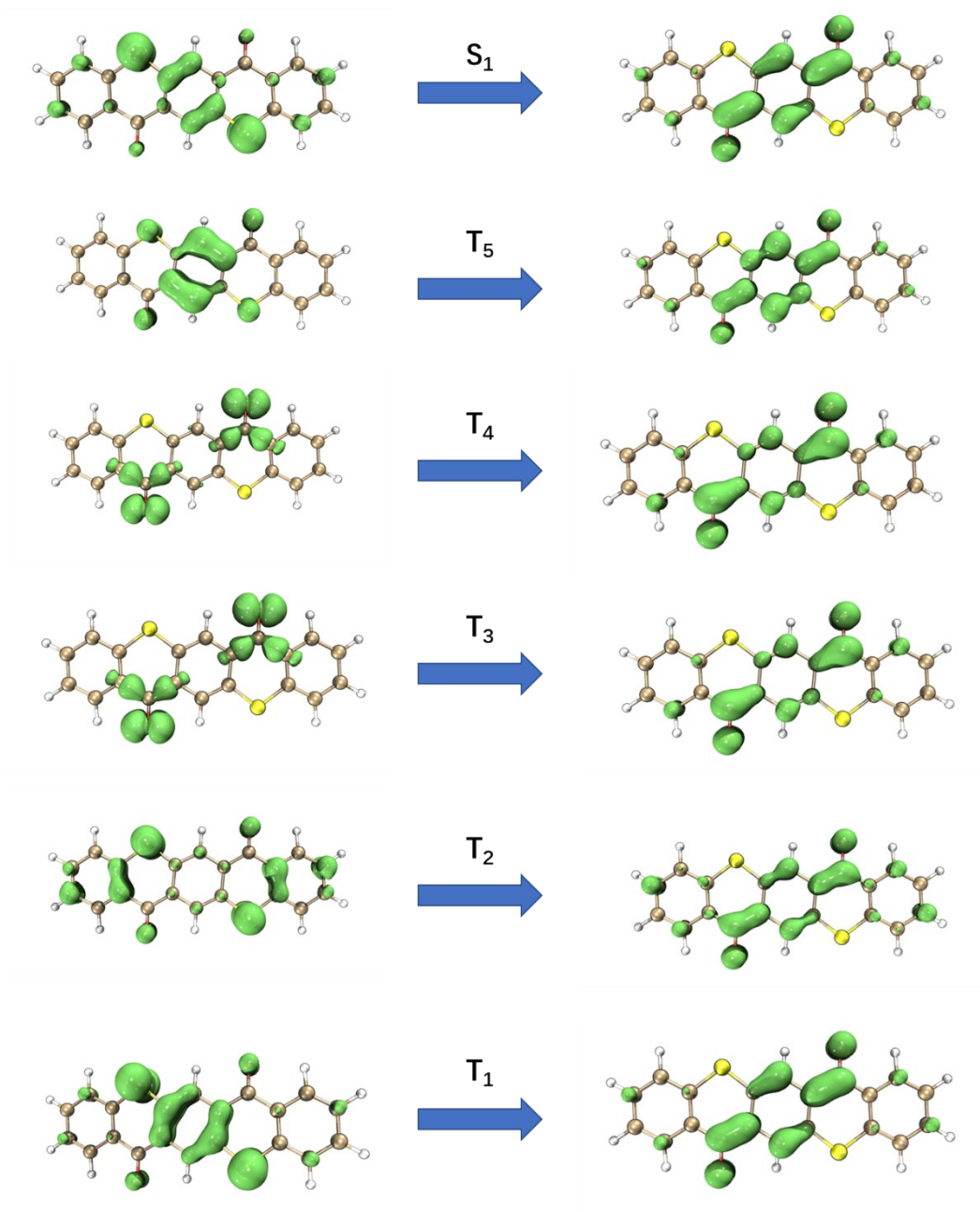
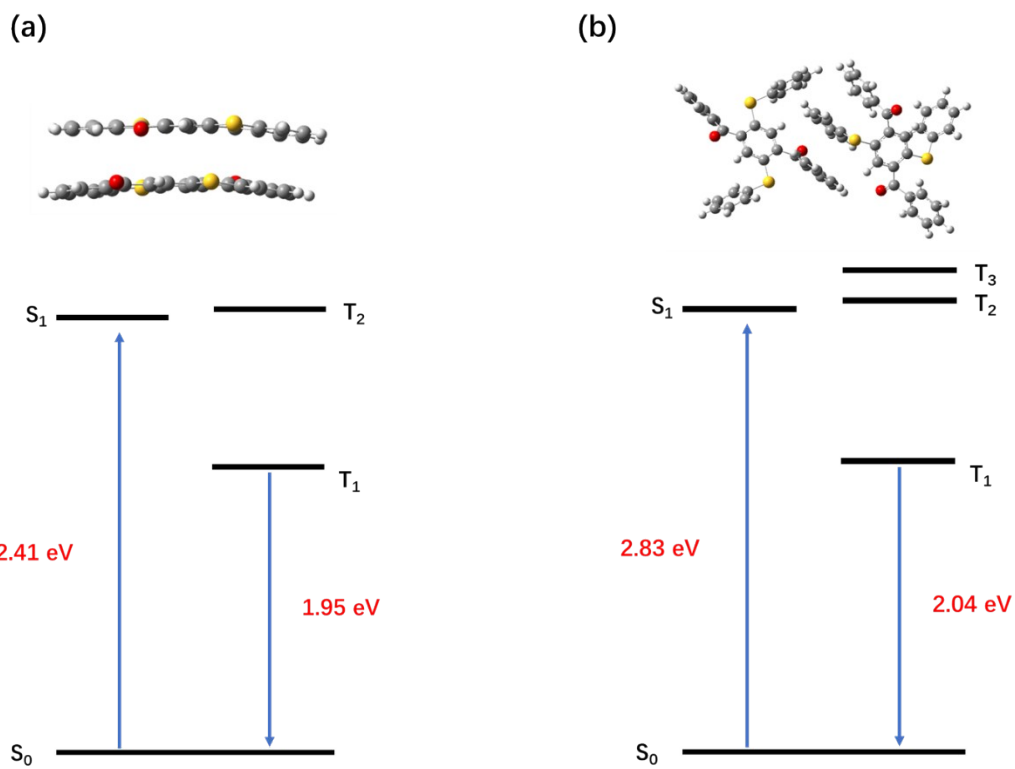**Fig. S4** The hole and electron distributions of FBPSP.

Fig. S5 The hole and electron distributions of BPSP.

LUMO	**-1.72 eV**		**-0.89 eV**
	↑		↑
	5.24 eV		**6.02 eV**
	↓		↓
HOMO	**-6.96 eV**		**-6.91 eV**
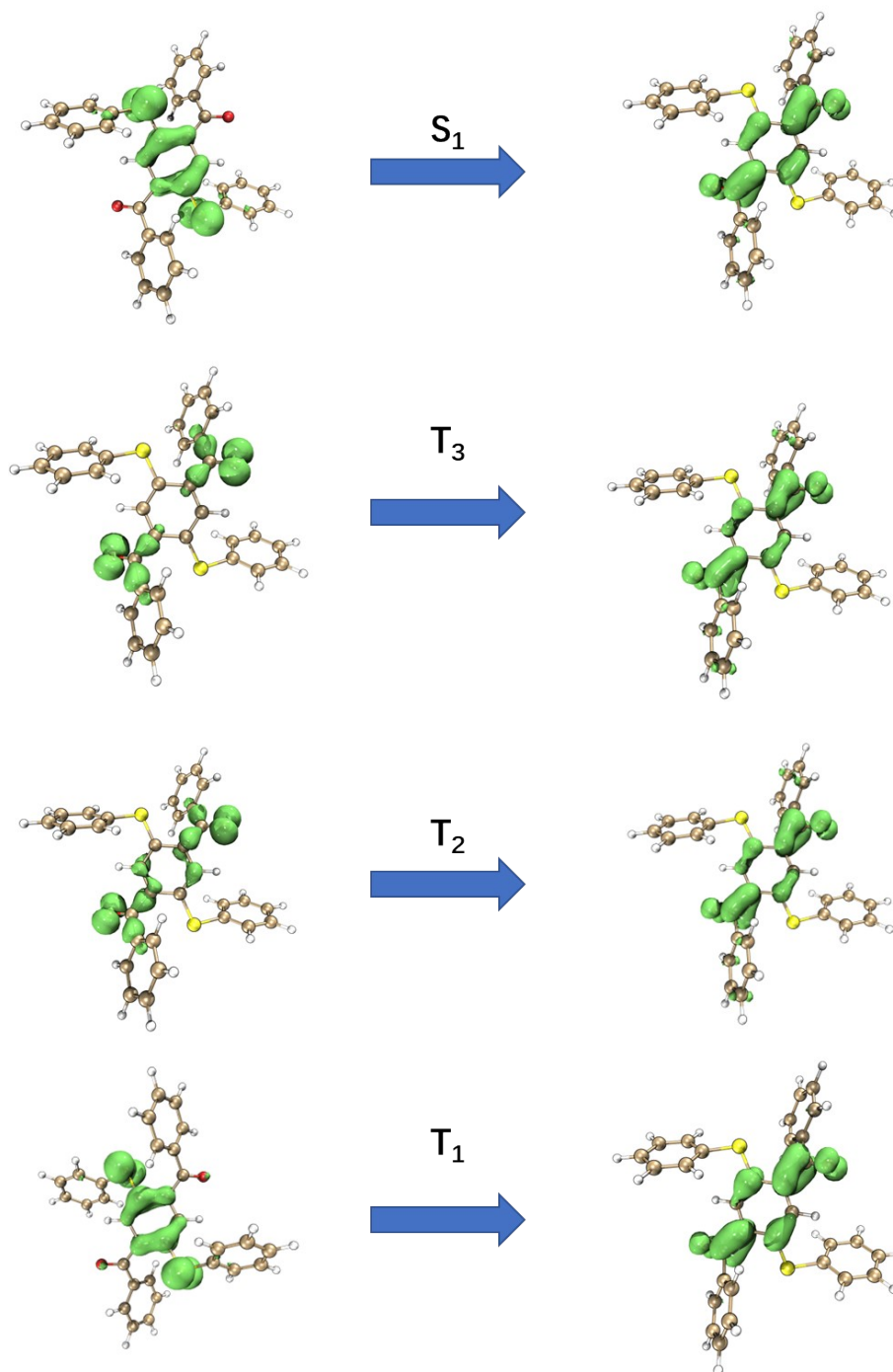
FBPSP   **BPSP**

**Fig. S6** Frontier molecular orbital distributions of FBPSP dimer and BPSP dimer.

Fig. S7 TD-DFT calculated excited states energies for (a) FBPSP dimer and (b) BPSP dimer at optimized T_1-geometry.

Table S9. The singlet and triplet excited state energies of FBPSP dimer at the optimized T_1-geometry. $T_n < S_1+0.3$ eV were marked in light green.

Excited state	Energy (eV)	Energy gap (S_1-T_n) (eV)
S_1	2.4072	
T_1	1.9521	0.4551
T_2	2.4980	-0.0908
T_3	2.9029	-0.4957

Table S10. The singlet and triplet excited state energies of BPSP dimer at the optimized T_1-geometry. $T_n < S_1+0.3$ eV were marked in light green.
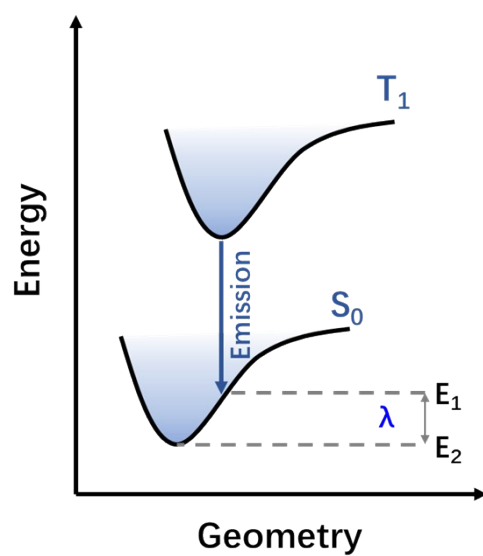
Excited state	Energy (eV)	Energy gap (S_1-T_n) (eV)
S_1	2.8263	
T_1	2.0357	0.7906
T_2	2.9098	-0.0835
T_3	2.9700	-0.1437
T_4	3.1859	-0.3596
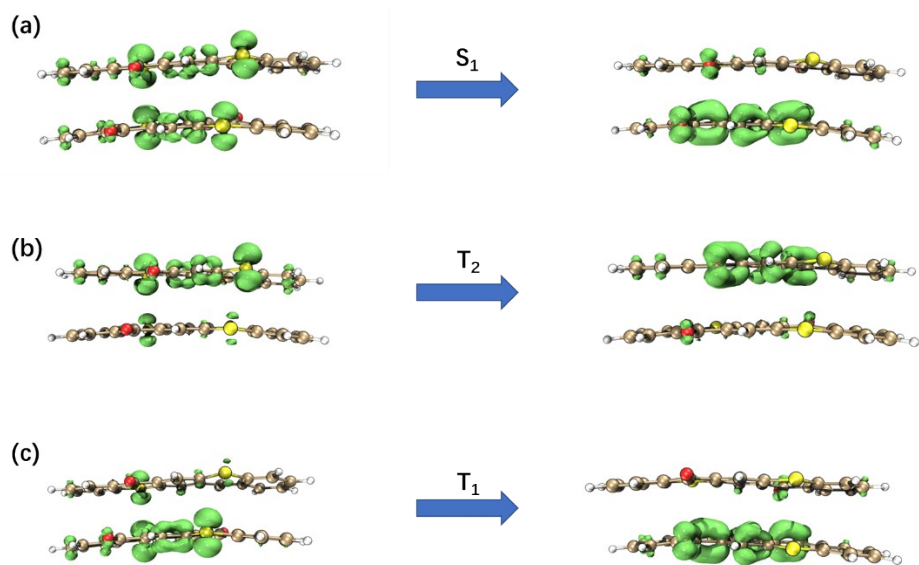
Fig. S8 The hole and electron distributions of FBPSP dimer.

(a) S₁

(b) T₃

(c) T₂

(d) T₁
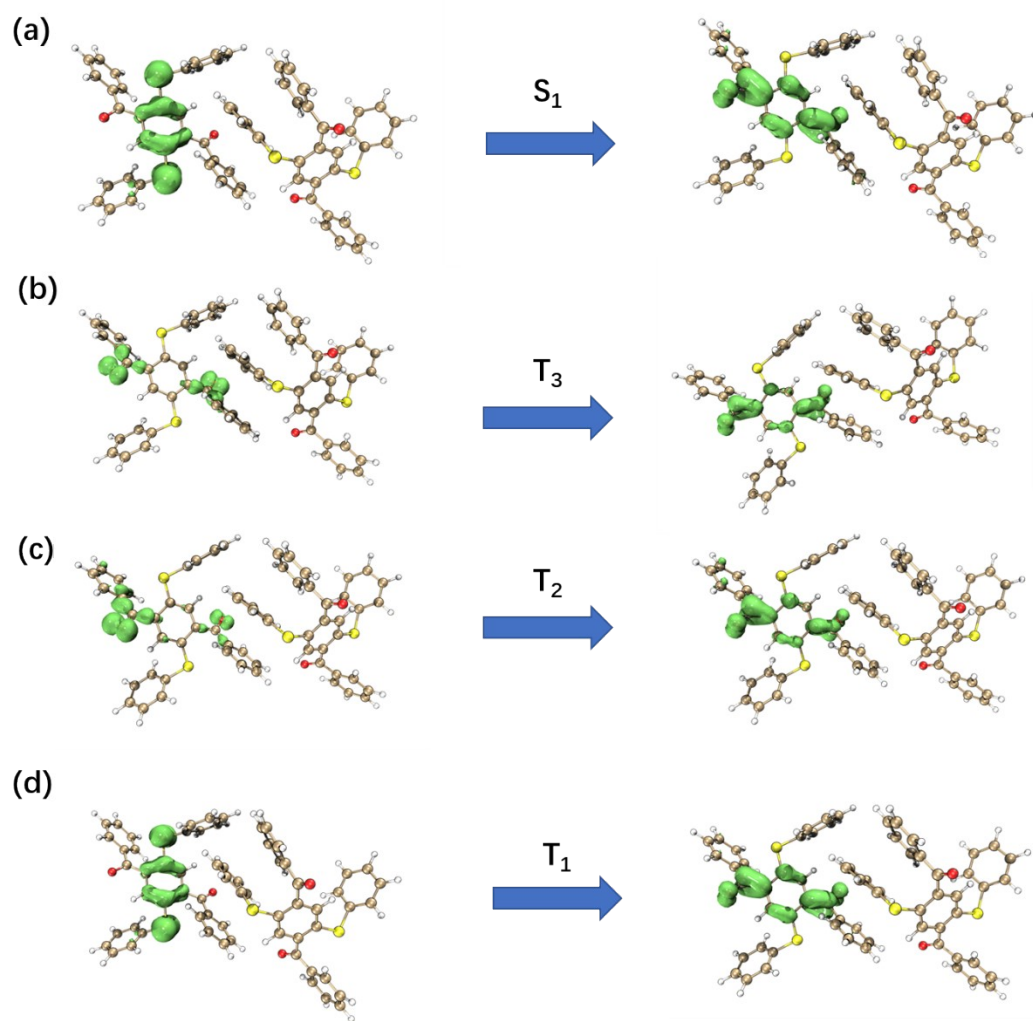
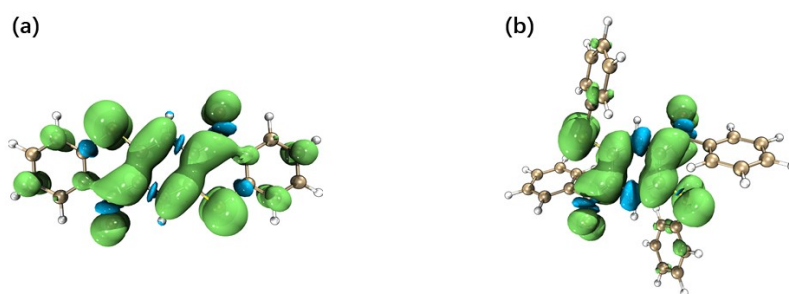**Fig. S9** The hole and electron distributions of BPSP dimer.

Figure S10. Diagram of energy level for FBPSP and BPSP.

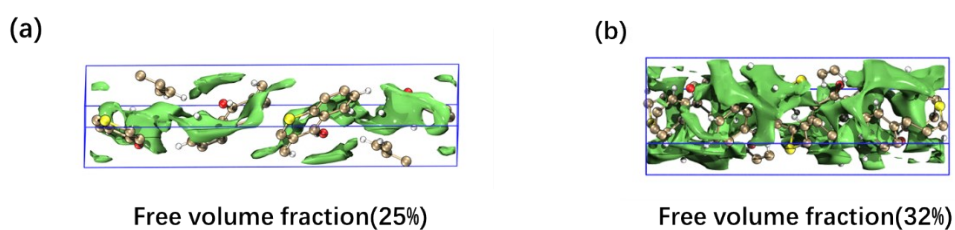**Table S11.** The energy of FBPSP and BPSP[9].

	E_1 (eV)	E_2 (eV)	λ (eV)
FBPSP	-46631.62	-46631.86	0.24
BPSP	-59254.49	-59255.06	0.57

$\lambda = E_1 - E_2$

Fig. S11 The SDD of T_1 states of (a) FBPSP and (b) BPSP.

Free volume fraction(25%)   Free volume fraction(32%)

Fig. S12 The free volume fraction of (a) FBPSP and (b) BPSP.
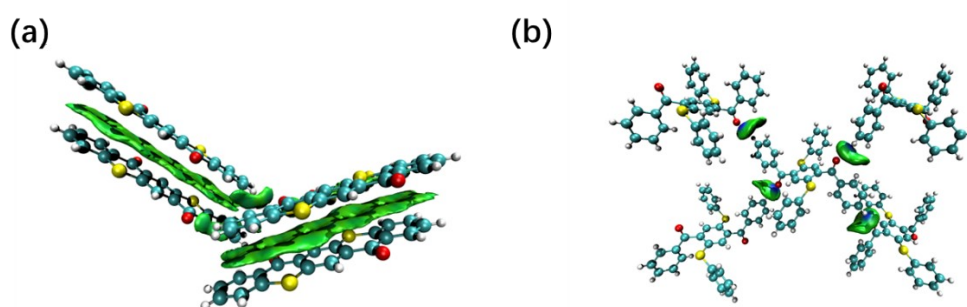
Fig. S13 The calculated molecular interactions (green isosurface) in (a) FBPSP and (b) BPSP crystal.
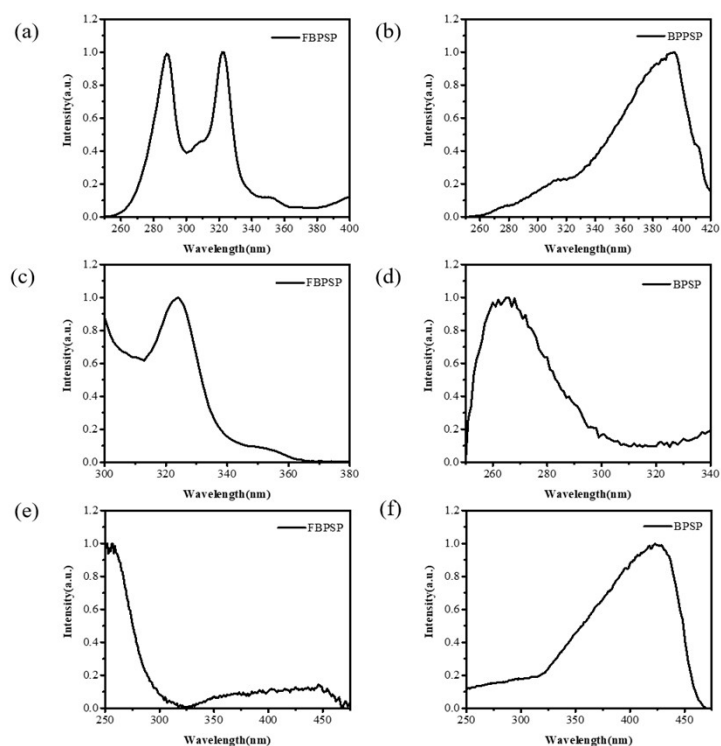
Fig. S14 Excitation spectra of (a) FBPSP and (b) BPSP at room temperature in THF solution (10 μM). Excitation spectra of (c) FBPSP and (d) BPSP in doped film at room temperature in vacuo. Excitation spectra of (e) FBPSP and (f) BPSP in in crystal at room temperature under air.

5. Reference

1. S. Wang, H. Shu, X. Han, X. Wu, H. Tong and L. Wang, *J. Mater. Chem. C*, 2021, **9**, 9907-9913.
2. R. Huang, J. S. Ward, N. A. Kukhta, J. Avo, J. Gibson, T. Penfold, J. C. Lima, A. S. Batsanov, M. N. Berberan-Santos, M. R. Bryce and F. B. Dias, *J. Mater. Chem. C*, 2018, **6**, 9238-9247.
3. Y. Li, L. Jiang, W. Liu, S. Xu, T. Y. Li, F. Fries, O. Zeika, Y. Zou, C. Ramanan, S. Lenk, R. Scholz, D. Andrienko, X. Feng, K. Leo and S. Reineke, *Adv. Mater.*, 2021, **33**, 2101844.
4. M. J. Frisch, G. W. Trucks, H. B. Schlegel, G. E. Scuseria, M. A. Robb, J. R. Cheeseman, G. Scalmani, V. Barone, B. Mennucci, G. A. Petersson, H. Nakatsuji, M. Caricato, X. Li, H. P. Hratchian, A. F. Izmaylov, J. Bloino, G. Zheng, J. L. Sonnenberg, M. Hada, M. Ehara, K. Toyota, R. Fukuda, J. Hasegawa, M. Ishida, T. Nakajima, Y. Honda, O. Kitao, H. Nakai, T. Vreven, J. A. Montgomery, Jr., J. E. Peralta, F. Ogliaro, M. Bearpark, J. J. Heyd, E. Brothers, K. N. Kudin, V. N. Staroverov, T. Keith, R. Kobayashi, J. Normand, K. Raghavachari, A. Rendell, J. C. Burant, S. S. Iyengar, J. Tomasi, M. Cossi, N. Rega, J. M. Millam, M. Klene, J. E. Knox, J. B. Cross, V. Bakken, C. Adamo, J. Jaramillo, R. Gomperts, R. E. Stratmann, O. Yazyev, A. J. Austin, R. Cammi, C. Pomelli, J. W. Ochterski, R. L. Martin, K. Morokuma, V. G. Zakrzewski, G. A. Voth, P. Salvador, J. J. Dannenberg, S. Dapprich, A. D. Daniels, O. Farkas, J. B. Foresman, J. V. Ortiz, J. Cioslowski, and D. J. Fox, Gaussian 09, Revision D.01, Gaussian, Inc., Wallingford CT, 2013.
5. U. Ekstrom, L. Visscher, R. Bast, A. J. Thorvaldsen and K. Ruud, *J. Chem. Theory Comput.*, 2010, **6**, 1971-1980.
6. T. Lu and F. Chen, *J. Comput. Chem*., 2012, **33**, 580-592.(Multiwfn).
7. Z. Shuai, *Chinese J. Chem.* **2020**, *38*, 1223-1232.
8. Z. Shuai, Q. Peng, *Phys. Rep.* **2014**, *537*, 123-156.
9. H. Zhu, I. Badía-Domínguez, B.Shi, Q. Li, P. Wei, H. Xing, M. C. R. Delgado and F. Huang, *J. Am. Chem. Soc.*, 2021, **143**, 2164-2169.